

Contact resistance: the return of the Cox and Strack method for heterojunction solar cells

By:

Mateo Estrada Jorge

A THESIS

Submitted to

Oregon State University

In partial fulfillment of the
requirements for the degree of

Bachelor of Science

Submitted on May 10, 2019

Oregon State University Advisor: Dr. Ethan Minot

Arizona State University Advisor(s): Dr. Zachary Holman & William Weigand

Table of contents

Abstract

1 – Introduction

1.1 Motivation and Objective

1.2 Components of resistance in solar cells

1.2.1 Series resistance

1.2.2 Contact resistance for Cox and Strack

1.2.3 Contact resistance for transfer length

1.3 Heterojunction

1.3.1 Passivation

1.3.2 Transparent conductive oxides

2 – Methods

2.1 Transfer length method

2.1.1 Developing the TLM samples

2.1.2 Measuring the contact resistance

2.2 Cox and Strack method

2.2.1 Developing C/S method samples

2.2.2 Measuring the contact resistance

3 – Results:

3.1 TLM measurements

3.1.1 TLM: I-V lines

3.1.2 TLM: pad spacing versus total resistance

3.2 C/S method measurements

3.2.1 C/S: I-V lines for C/S method

3.2.2 C/S: inverse area versus total resistance

3.3 Discussion

3.2.3 Comparing the two methods

4 Conclusion

List of figures

FIG. 1: RESISTANCE DIAGRAM FOR THE VARIOUS COMPONENTS PRODUCING A CONTACT RESISTANCE IN A SOLAR CELL PROTOTYPE. (TAKEN FROM SCHRODER).....	7
FIG. 2: THE SETUP USED TO SOLVE FOR THE EQUATION USED TO GET THE CONTACT RESISTIVITY FOR TLM.	9
FIG. 3: THE BANDGAP BETWEEN ITO (N+) AND A-SI H(P).....	11
FIG. 4: BARRIER HEIGHT AND WIDTH AND CONDUCTION MECHANISM FOR METAL-SEMICONDUCTOR CONTACTS WITH INCREASING SEMICONDUCTOR DOPING CONCENTRATION (TAKEN FROM SCHRODER).	12
PHOTO 1: MEASURING THE TOTAL RESISTANCE WITH THE TLM METHOD USING A KEITHLEY DEVICE.....	14
FIG. 5: TOP VIEW OF THE PADS AND THE PROBING METHOD TO MEASURE AN I-V CURVE WITH THE KEITHLEY FOR TLM METHOD.	14
FIG. 6: CIRCULAR PATTERNS MADE ON A DUMMY WAFER MASK TO BE USED ON THE SAMPLES TO DEPOSIT THE ITO.	16
FIG. 7: TOP VIEW OF C/S SAMPLES WITH CIRCULAR CONTACTS OF KNOWN DIAMETER.	16
FIG. 8: C/S MODEL FOR MEASURING THE CONTACT RESISTANCE THROUGH THE SAMPLES. C-SI WAS $\sim 150\text{ }\mu\text{M}$, A-SI $\sim 8\text{NM}$, AG AT $250\text{ }\mu\text{M}$, AND ITO AT $\sim 80\text{ }\mu\text{M}$	17
TABLE 1: SUMMARY OF THE DOPANT, TCO MATERIALS: ITO, IO, AND IZO, AND THE CONCENTRATION OF OXYGEN AND THICKNESS OF EACH MATERIAL.	18
FIG. 9: TLM: I-V LINES FOR ITO. I-V CURVES FOR AN ITO SAMPLE WITH TLM AND INCREASING DISTANCE BETWEEN CONTACT PADS SHOWING RESISTANCE INCREASES AS THE DISTANCE BETWEEN PADS (S) INCREASE.....	19
FIG. 10: TOTAL RESISTANCE VS. DISTANCE. TOTAL RESISTANCE VERSUS THE PAD SPACING FOR THE TLM METHOD. THREE DIFFERENT TCO'S WERE USED.....	20
FIG. 11: I-V WITH C/S: I-V LINES FOR DIFFERENT CONTACT DIAMETERS WITH ITO WITH C/S METHOD.	21
FIG. 12: A-B-C: TOTAL RESISTANCE VERSUS THE INVERSE DIAMETER SQUARED OF THE CIRCULAR CONTACTS FOR: IO, IZO, AND ITO (IN THAT ORDER) USING THE C/S METHOD.....	22
FIG. 13: THE CONTACT RESISTIVITIES FOR ALL THE DIFFERENT TCO'S FOR THE TWO DIFFERENT MEASUREMENT METHODS.....	23

Abstract:

Solar photovoltaics are becoming a source of renewable energy for cities where sunlight is abundant. The efforts to increase their efficiency ranges from increasing the number of P-N junctions, to new methods for decreasing resistivity between semiconductors and metals. In this work, we focus on methods to characterize contact resistance with semiconductors between 200-150 μm . The long-term goal will be to reliably apply one of the methods, Cox and Strack (C/S), to semiconductor materials of less than 150 μm . Cox and Strack, were researchers in the sixties whose method for measuring contact resistance in transistors paved the way for figuring out how to make transistors more efficient. Since then, no one has attempted this new method for solar cells. In my paper, I developed and tested a revised version of their method for solar cells. My method was tested in parallel with the standard method for measuring contact resistance in solar cells to test if the new method was reliable in solar cells. The C/S method measures contact resistance through the heterojunction, whereas TLM relies on a lateral measurement. The results indicated a potential application for TCOs whose bandgap “aligns” with silicon, my data indicates ITO to be the best candidate. The TLM data was inconclusive and thus wasn’t of use to compare it to the C/S data. However, previous experiments have shown contact resistance to be within the range of the measured contact resistance with the C/S method from my experiment. This experiment lays groundwork for future applications in successfully building less contact resistive heterojunction solar cells which could be up to 30% efficient. It promises to be in direction for increasing efficiency of solar cell technology.

1 Introduction

1.1 Motivation and Objective:

The photovoltaic effect is a physical phenomenon occurring when electrons interact with photons to produce a current. It's applications in electronics extend beyond solar cells, it's used in other semiconductor device research like diodes, LED, and transistors. Solar cells are used as an alternate renewable energy source for generating electricity. Its applications in satellite and other aerospace related devices are what drove research for generating more efficient solar devices [1]. Solar cells are built of many intricate components which are crucial to making them efficient. However, my research is the resistance aspect of it, specifically measurements of contact resistance. Contact resistance is one of multiple components of total series resistance.

Series resistance lowers the overall efficiency of solar cells, meaning it decreases the maximum power output. In single junction solar cells contact resistance between metals and semiconductors is negligible. However, in multiple-junction cells contact resistance becomes a problem [2]. Contact resistance decreases the amount of electron-hole interactions, thus reducing output current, voltage, and power. The negative effects of contact resistance on solar cell efficiency for heterojunction cells make it a topic of further research. As methods for decreasing it will in the long term increase overall efficiency of tandem solar cells [2]. Thus, contact resistance will be the primary focus of my thesis.

The main component I studied was contact resistance between metals and semiconductors. The standard way of measuring contact resistance between metals and semiconductors is called the transfer length method (TLM) and is used in semiconductors 100-200 μm thick. There are complications when attempting to measure the contact resistance for semiconductors thinner than this due to spreading of current in thinner devices (Fig 1) [3]. My goal was to develop a method for measuring contact resistance on solar cells which measures contact resistance beyond the measuring capabilities for TLM. Due to the disadvantages of measuring contact resistance in thinner semiconductors. The new method was studied by Juan Asencio and me at Arizona State University over summer of 2018. The new method was an implementation of a method used by Cox and Strack (C/S). This method was developed in an attempt to measure contact resistance of transistors in the 1960s. My research is an extension of C/S methodology for solar cells [2].

1.2 Components of resistance in solar cells:

Before getting into the experimental work, it's important to know how solar cells work at a fundamental level. In solar cells, the photovoltaic effect is used via the fact that light interacts with matter quantum mechanically [1]. In a solar cell, a P-N junction helps to increase the amount of time an electron is above its ground state energy level, after being excited by a photon whose energy is equal to or above its band gap energy, consequently the electron can be transported by a conductor [1]. The P-N junction is made with a semiconductor which is manufactured to have a P region (holes) and an N region (electrons). The P region has electrons missing in its atomic structure, which means it will accept electrons from wherever it can get them, the N region has excess electrons and the idea is to use electrons moving with respect to time to make a current, by definition ($\frac{dQ}{dt} = I$). The current is captured by a conductive metal structure soldered at the top of the solar cell; these are called the busbars (Fig. 1).

1.2.1 Series resistance

Series resistance is divided into three main components: contact resistance between semiconductor and metal, resistance in the movement of current from base to emitter, and resistance from the front and rear metal contacts which collect the current being generated by the photovoltaic effect [3]. The focus will be resistance at the interface between metal and semiconductor, where the new C/S method will be used for measuring contact resistance. TLM will be used to compare the two results (see discussion). The method for measuring the contact resistance with TLM is to plot the total resistance versus pad distance. The y-intercept of the trendline should be the contact resistance [3].

The various components which provide a resistance to a solar cell can be seen below. The main components studied in the following experiment are: R_1 , R_2 , R_3 , and R_4 . This is where the contact resistance occurs, and the experimental setup will not have the busbars (R_6) or the gridlines (R_5) to reduce uncertainty and because it's not important for the measurements [3].

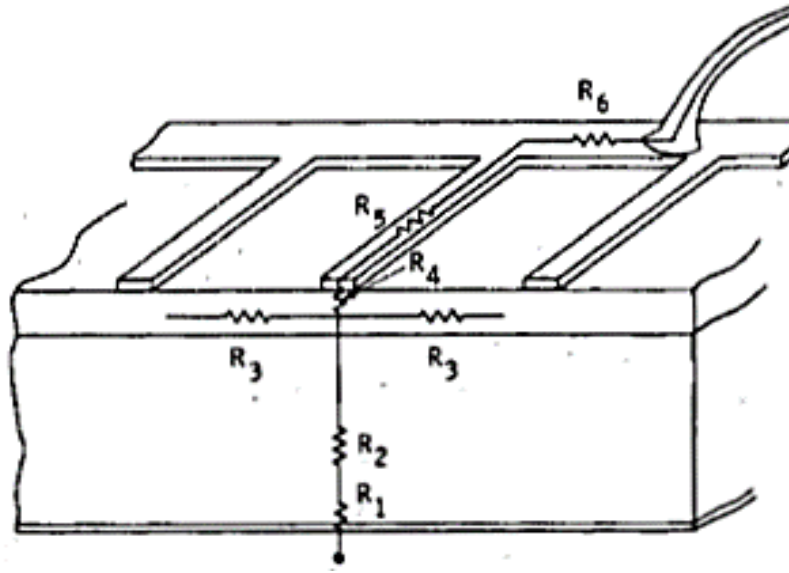


Fig. 1: Resistance diagram for the various components producing a contact resistance in a solar cell prototype. (Taken from Schroder).

R_1 = Back Contact

R_4 = Front Contact

R_2 = Bulk

R_5 = Grid Lines

R_3 = Diffused layer

R_6 = Bus lines

1.2.2 Contact resistance for Cox and Strack

The total spreading resistance which will be present at the interface between the metal and semiconductor for the new method will be defined by equation (1) [4].

$$R_T = \frac{\rho}{d\pi} \arctan\left(\frac{4t}{d}\right) + \frac{4R_c}{\pi d^2} + R_0 \quad (1)$$

t: thickness of the diffused layer

d: contact diameter

R_c : specific contact resistance

R_0 : residual resistances due to the substrate or the resistances from the back side

ρ : resistivity of multilayer setup

I will design contacts in a circular shape because the arctan term is only defined for spreading resistances for circular contacts [2]. The method to figure out arctan term was made by C/S via an electrolytic tank experiment [2]. To extract the contact resistance, Equation (1) can be solved for R_c which yields;

$$\frac{4R_c}{\pi d^2} = R_T - \frac{\rho}{d\pi} \arctan\left(\frac{4t}{d}\right) - R_o, \quad (2)$$

if we let the R_o be negligible, and take into account the fact that $t \ll d$, because the thickness of the A-Si is in the range of microns, the arctan can be simplified to:

$$\frac{\rho}{d\pi} \arctan\left(\frac{4t}{d}\right) \approx \frac{4t\rho}{\pi d^2} \quad (3)$$

Which yields a simpler equation,

$$R_T = \frac{4R_c}{\pi d^2} + \frac{4t\rho}{d^2\pi} \quad (4)$$

And if we factor πd^2 the new R_c is:

$$R_c = \frac{\pi d^2}{4} \left(R_T - \frac{4t\rho}{d^2\pi} \right) \quad (5)$$

This equation is used to figure out the contact resistivity for the C/S method, since t is small, the first term is the most useful. However, the adapted method to get this term involved three steps: measure I-V curves for the C/S samples, take the slope of these curves to get total resistance, and plot the total resistances (R_{total}) versus the inverse pad area ($1/A$). The slope of R_{total} vs. $1/A$, will be the specific resistivity (R_T) from equation (4). The wafers have a contact resistivity of $\sim 3 \text{ Ohm}\cdot\text{cm}^2$, (ρ), and a thickness, (t), of $177 \text{ }\mu\text{m}$, the contact resistance will be calculated using Equation (5).

1.2.3 Contact Resistance for transfer length

Contact resistance will depend on the type of semiconductor, metal, and mostly on the dopant at the surface of the semiconductor [3]. This implies low values of dopant lead to high values of contact resistance, and high dopant density means lower contact resistivity (Fig. 3). Measuring contact resistance can be done with TLM for devices which display ohmic contact properties. The idea behind TLM is of sending a current and voltage through the device as is shown in Fig 4. After capturing the I-V curve, the slope of the I-V curve will indicate if there is ohmic behavior of the tested samples. If the slope is linear, then the samples work and the TLM can be used to calculate the contact resistance. Ohmic contacts allow flow of current from a semiconductor to a metal and vice versa and having linear I-V curves is necessary as seen from previous experiments for measuring contact resistance [3].

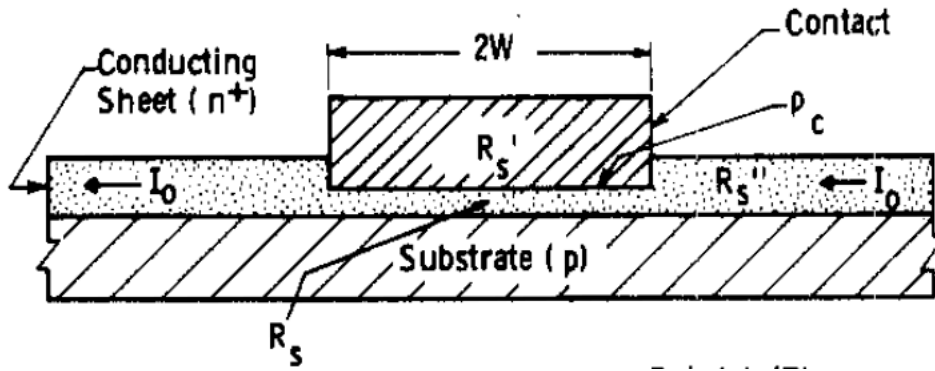


Fig. 2: The setup used to solve for the equation used to get the contact resistivity for TLM.

The differential equation is taken from the Fig. 2 by using Kirchhoff's current and voltage law,

$$\frac{d^2}{dx^2} I_2(x) - \frac{\rho_c}{R_s + R_s'} I_2(x) = -\frac{R_s'}{\rho_c} I_0, \quad (6)$$

using boundary conditions to define the solution:

$$I_2(x = W) = I_0, \quad (7a)$$

$$I_2(x = -W) = I_0 \quad (8b)$$

leading to the solution;

$$I_2(x) = \frac{I_0 R_s}{R_s + R'_s} \left[\frac{R'_s}{R_s} + \frac{\cosh\left(\frac{x}{a}\right)}{\cosh\left(\frac{w}{a}\right)} \right] \quad (9)$$

Since the measurement of contact resistance for this method is done via a current and voltage input, an integral is required to see how the voltage drops along between the contact pads (Fig. 5). The integral is;

$$\Delta V_{bar} = \int_{-w}^w I_2(x) R_s \frac{dx}{z} \quad (10)$$

Along with the gap between adjacent contact bars, the final equation giving the voltage drop between pads is;

$$V_{AB} = \left(\frac{n I_0 R_s}{z} \right) (S + 2L_T) \quad (11)$$

Where:

n: number of contact pads

R_s : sheet resistance

I_0 : input current

S: pad spacing

L_T : the characteristic distance over which current transfer occurs

To figure out the contact resistivity ρ_c , it's necessary to solve for the sheet resistivity R_s and have the pad spacings (S). After obtaining the sheet resistance, solving for the current transfer length L_t , is simply found by getting the y-intercept of the graph made from (R_s) vs. (S). Finally, applying the known variables to Equation (12) to solve for the contact resistivity [3]:

$$\rho_c = R_s L_t^2 \quad (12)$$

1.3 Heterojunction:

In solar photovoltaics, a heterojunction is a structure whose multilayers of different crystalline semiconductors vary in their bandgap energy [5]. This makes it so a broader range of photons can be captured via the photovoltaic effect. Heterojunction cells are also some of the most efficient solar cells produced in industry due to their photon capturing properties [5]. The bandgap between ITO and A-Si (n-type) to illustrate the amount of energy from a photon an electron needs to jump from the valence band to the conduction band (Fig. 3). When an electron is free of its bound state, it can quantum tunnel to the ITO and up into the Ag to be collected as current (Fig. 3). In my experiment, the semiconductor is silicon and there will be two different layers of amorphous-silicon at different densities (Table 1) on top of the main silicon structure. This will serve as the main passivation structure.

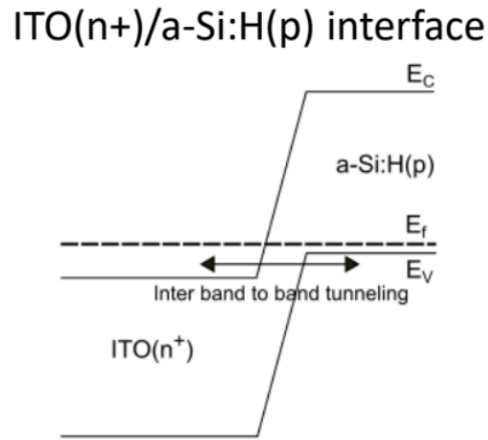


Fig. 3: The bandgap between ITO (n+) and A-Si H(p).

1.3.1 Passivation

The reason for using the amorphous silicon layers between the silicon and the TCO is to passivate the surface. When electron-hole pairs are generated by the photovoltaic effect, they travel on the surface to be collected as current by the busbars (Fig. 1). However, imperfections at the surface will trap electron-hole pairs causing them to recombine [6]. The photovoltaic effect generates an electron-hole pair after silicon atoms are excited by incoming photons causing the quantized electrons to jump to a higher energy state due to the electron-photon interactions commonly known as photoelectric effect. Recombination happens because electron-hole pairs are recombined due to molecular impurities at the silicon surface. These molecular impurities are unevenly charged at the surface of the silicon thus making the electron-hole pairs recombine to

neutralize the uneven charge distributions of the silicon surface. The dopant we used is amorphous silicon and in Fig. 4 the bandgap diagram is shown for lower to higher doping densities [3].

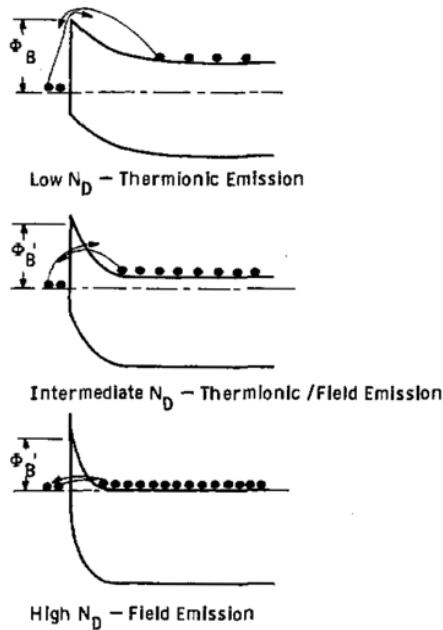


Fig. 4: Barrier height and width and conduction mechanism for metal-semiconductor contacts with increasing semiconductor doping concentration (Taken from Schroder).

1.3.2 Transparent Conductive Oxides:

Transparent conductive oxides (TCO) were used as the metal contact between the silicon and the silver contact at the top of the samples. These TCOs are crucial in making sure the band-gap's align so electron-hole pairs can flow “easily” between the interfaces of metal and semiconductor [3]. I used ITO (indium-tin oxide), IZO (indium-zinc-oxide) and IO (indium oxide) as the main test subjects. The TCOs were deposited with a gas chamber (include model and make). The TLM samples will be made with specifications provided by Table 1. The samples are not fully functional solar cells, they are a design to test how the electrons will get out from the crystalline silicone.

2 Methods

2.1: Transfer length method:

TLM is the main form of measuring contact resistance between transparent conductive oxides (TCO) and semiconductors. The idea behind this method is of sending a current (I) and voltage (V) into a contact pad with a Keithley device (Keithley Instruments 2450 SourceMeter) with a four-point probe to collect an I-V lines (Fig. 4). The four-point probe method is done by measuring the voltage between two probes and the current between the other two probes. This limits the outside resistive effects because it limits the path of the voltage and current to two probes. If the I-V curve collected with the Keithley device is linear, an ohmic contact is shown. This is shown in Fig. 9 for the TLM samples.

For the purposes of this research, probe 1 (current in) and probe 2 (voltage in) will be sent through the Ag, ITO, and into the layers of A-Si. Theoretically, I_{in} and V_{in} will flow laterally in the C-Si(n) and will complete the contact with probes 4 (I_{in}) and 5 (V_{out}) measure voltage and current drops to yield I-V curves [3].

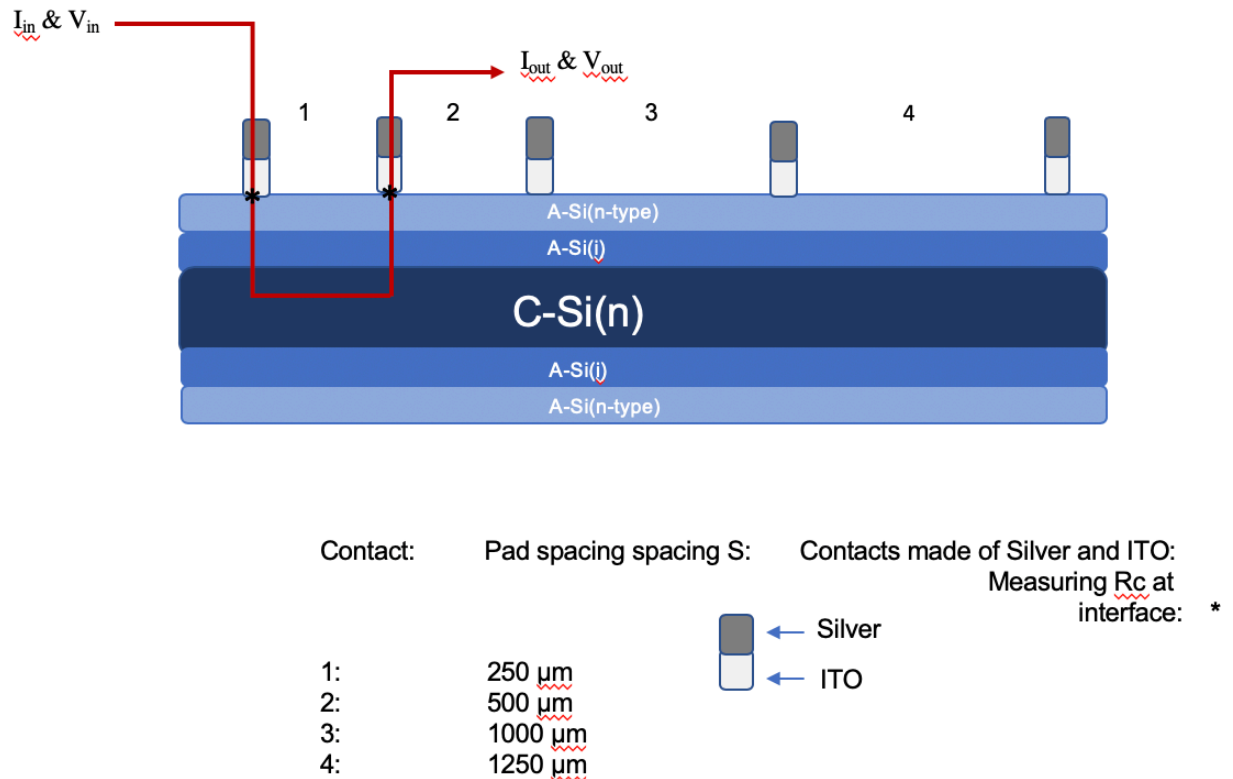


Fig. 4: A-Si (i) on a silicon semiconductor with a TCO for passivation and a silver contact for current conduction and measurement using the TLM method.

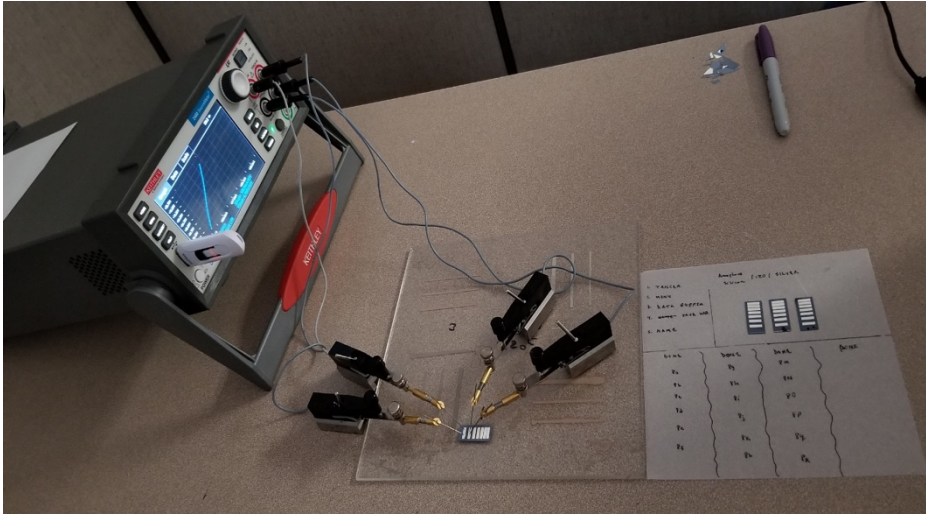


Photo 1: Measuring the total resistance with the TLM method using a Keithley device.

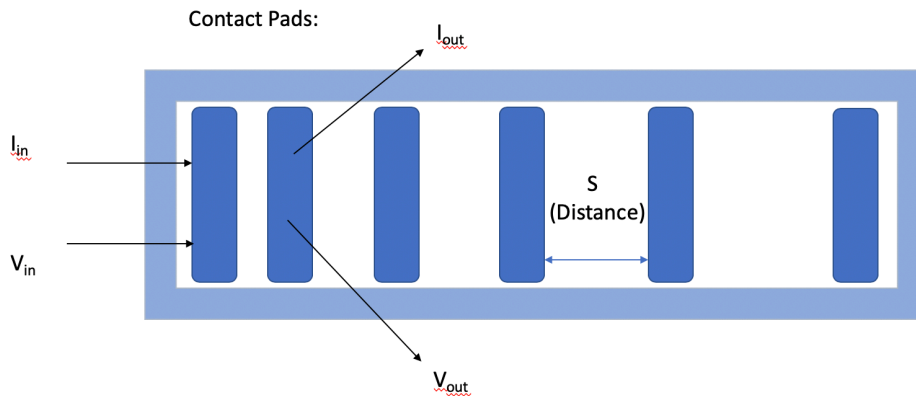


Fig. 5: Top view of the pads and the probing method to measure an I-V curve with the Keithley for TLM method.

This method is conventional for most semiconductor devices like solar cells, transistors, etc. The contact resistance should change as the distance between the contact pads changes. However, before measuring contact resistance between ITO and Ag in this case, ohmic contacts needs to be confirmed. To confirm its presence, measurements should present a linear I-V curve, the slope of which will supply the total resistance of the sample. If the device has a linear trend it will indicate that the interface between metal and semiconductor is indeed ohmic.

2.1.1: Developing the Samples for TLM:

The samples were built in collaboration with Arizona State University graduate research assistant Will Weigand, who provided the doping on a silicon wafer via plasma deposition. He deposited two layers of amorphous silicon: one of A-Si intrinsic and the other A-Si n-doped, (see table 1). My task was to develop the other layers of the sample solar cell. To begin the process, I had to develop masks which made the contacts in circular shapes using dummy wafers made of silicon to limit contamination. I lasered (using an electrox EMS¹⁰⁰) the shapes onto these dummy wafers and made sure they were homogenous by looking at their surface with a microscope. I also cleaned them of burnt and uneven microscopical edges using a chemical bath of KOH. Using a plasma gas chamber (PVDO2) and the masks taped onto the heterojunction cell sample, ITO was deposited at about 80nm. The silver was deposited in a similar manner; however, the silver was thinner ~ 300nm as is shown in Table 1.

2.1.2: Measuring the Samples for TLM:

To measure the samples using the TLM, I will use the slopes measured from the I-V curves from Fig. 9. The slope from each I-V curve will yield the total resistivity plus the sheet resistance of the C-Si where the current will travel. Before measurements of contact resistivity are done, I will use Fig. 10 to confirm whether the total resistance versus the distance between contacts is linear, since it's not I will use the first three data points and find the y-intercept L_t , to solve for contact resistivity using Equation (6).

2.2: Cox and Strack method

The C/S method will be adapted for my samples as shown in Fig. 8. A current (I_{in}) and voltage (V_{in}) will flow in and a back plate will hold the sample on a vacuum seal, so the entire back of the sample is touching the plate. The plate will have the V_{out} and I_{out} plugged in to measure I-V curves using a setup of a Sinton Instruments FCT-450, a Keithley device (same as for TLM), and a LabVIEW program to connect the two.

2.2.1 Developing C/S method samples

The TLM for measuring contact resistance for heterojunction cells is useful when the semiconductors are thick (varying between 120-200 μm). However, for thinner semiconductors

this poses an issue given that the spreading current will leak from the sides of the semiconductor, and it will decrease the value of contact resistance to a threshold that is below what can be accurately measured with the TLM. The C/S method was introduced in the late 1960's as a way of measuring the contact resistance between a metal and a semiconductor in transistors. My method will involve developing a sample similar to Fig 5. However, there will be a measurement of the device from the top to the bottom as seen in Fig. 8. The techniques for the C/S method are: the semiconductor will include an ITO, Ag, and a passivation layer of A-Si (as shown in Fig 2), there will be circular contacts of varying diameter, and the measurements will have to be made using a 4-probe technique, further details will be discussed in results.

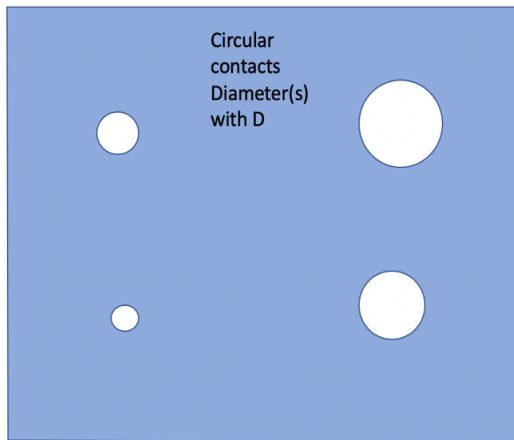


Fig. 6: Circular patterns made on a dummy wafer mask to be used on the samples to deposit the ITO.

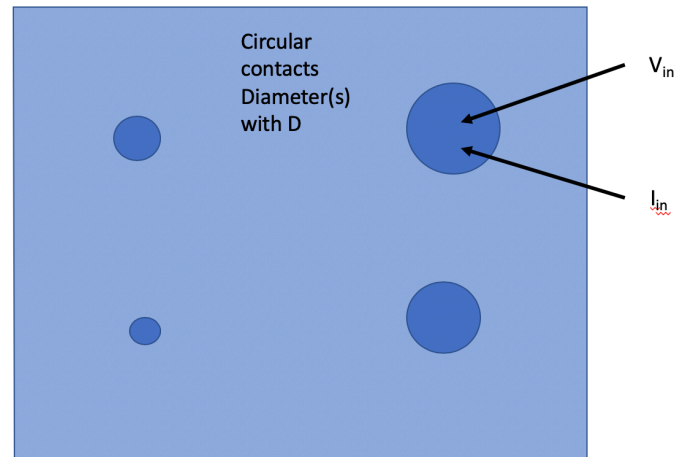


Fig. 7: Top view of C/S samples with circular contacts of known diameter.

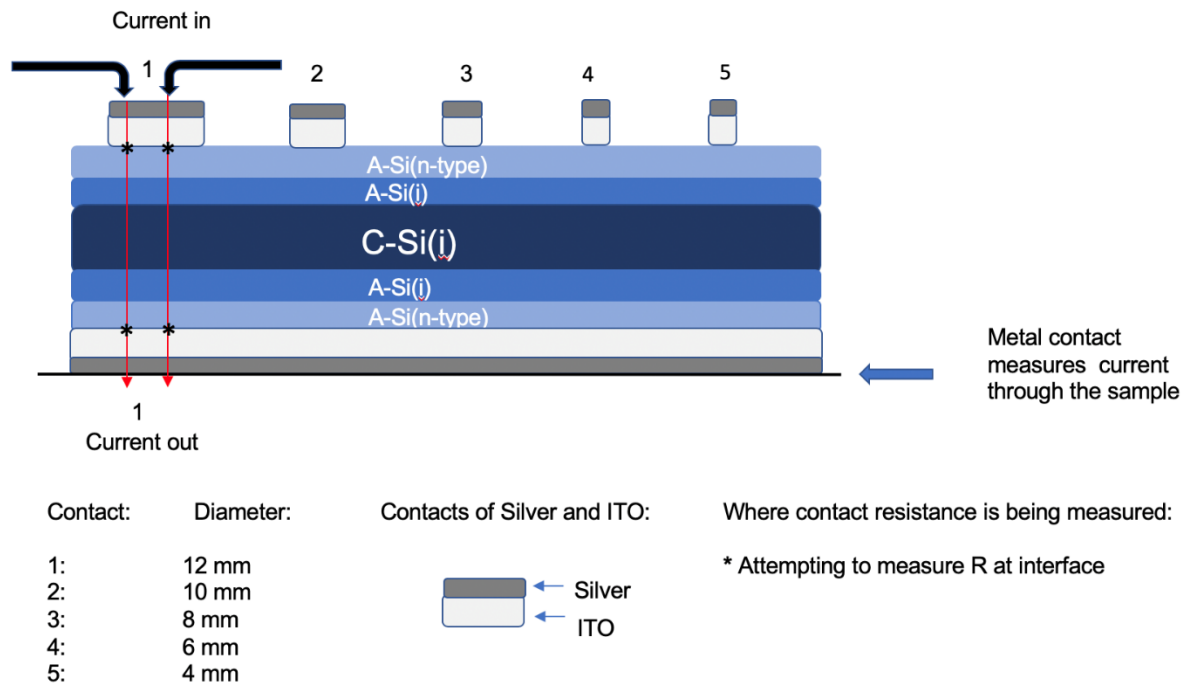


Fig. 8: C/S Model for measuring the contact resistance through the samples. C-Si was $\sim 150 \mu\text{m}$, A-Si $\sim 8\text{nm}$, Ag at $250 \mu\text{m}$, and ITO at $\sim 80 \mu\text{m}$.

The process for making the samples for the C/S measurements were similar to the TLM, with the exceptions of “dummy wafers” used to make masks to deposit the ITO ($\sim 80\text{nm}$) and silver onto the samples (see Fig. 7). However, for these samples I didn’t use rectangular shapes, instead I made the contacts circular. The circular shapes were motivated by the C/S paper for measuring contact resistance through devices. The silver was deposited in a similar manner; however, the silver was $\sim 300\text{nm}$ as is shown in Table 1. The back side of the heterojunction cell samples was also used to deposit ITO and silver as is shown in Fig 7. With the idea of making an ohmic contact at the other end of the cell, as this was important in making sure we were measuring resistance of the metal and semiconductor. To measure ohmic contact I used a four-point probing system which used two currents and a flat metal plate at the back end of the sample (photo 2).

	Thickness (t)	Doping
C-Si	~180 μm	n-type
A-Si:H(i)	8 nm	intrinsic
A-Si:H(n)	4.5 nm	n-type
TCO	80 nm	3% O ₂ , n-type
Ag	~300 nm	

Table 1: Summary of the dopant, TCO materials: ITO, IO, and IZO, and the concentration of oxygen and thickness of each material.

3 Results and Discussion

3.1 TLM measurements

3.1.1 TLM I-V lines:

Fig. 10 shows the current (I) versus Voltage (V). The different spacings are shown by the legend and indicate the change in the slope based on the spacings. The TCO for Fig. 9 was ITO and it was annealed for 20 minutes at 200 C⁰. Data trends of I-V lines before the samples' annealing were shown to be less linear than those taken after the annealing, making it more practical to measure.

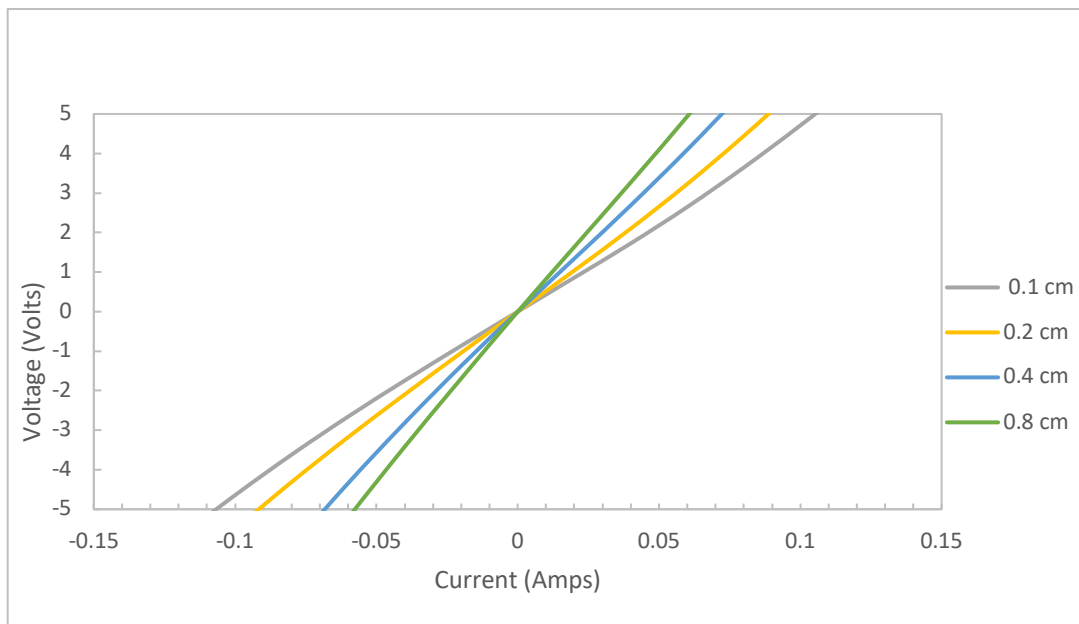


Fig. 9: TLM: I-V lines for ITO. I-V curves for an ITO sample with TLM and increasing distance between contact pads showing resistance increases as the distance between pads (S) increase.

After sweeping the I-V curve for each TCO with the transfer length method, the current and voltage were graphed as seen in Fig 9. This is was crucial for the data collection, because for TLM a linear slope is necessary to have attained an ohmic contact between ITO and A-Si (4). Since Fig. 9 shows the I-V curves using TLM as being linear, the total resistance of ITO sample can be found from the slope. This slope was then taken and plotted against the distance between each of the 4 contact pads (S).

3.1.2 TLM: pad spacing versus total resistance:

The contact resistance will be extracted from the intercept of the graph below. The Different samples of metal contacts: ITO, IZO, and IO, were used as test contacts. The total resistance in Ohms, versus the pad distance spacing is plotted to show how the total resistance changes as a function of the spacing [3]. The spacings increase and the contact pads were rectangular (Fig 5).

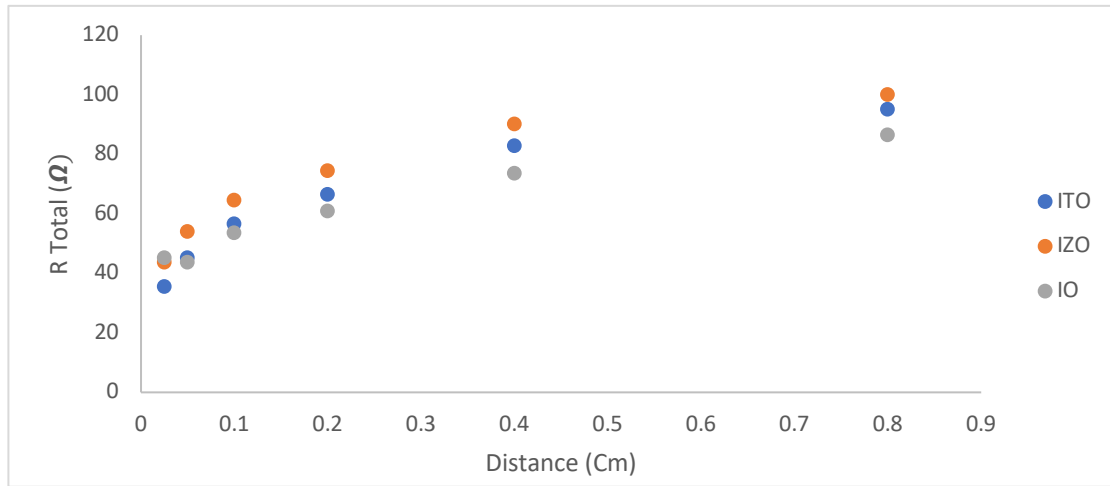


Fig. 10: Total Resistance vs. Distance. Total resistance versus the pad spacing for the TLM method. Three different TCO's were used.

The traditional method of figuring out the contact resistance for this method is to take the y-intercept of each TCO from Fig. 10 [2]. As the results gathered from the tests are non-linear, the data is inconclusive in regard to contact resistance for the contact pads used. Instead, the first three points for each TCO will be used to take the linear trend and use the line intercept as the contact resistance for the samples developed.

3.2 C/S method measurements:

3.2.1 C/S: I-V lines:

Below the I-V curves for the samples developed using the C/S method. The legend shows the diameter of each circular contact.

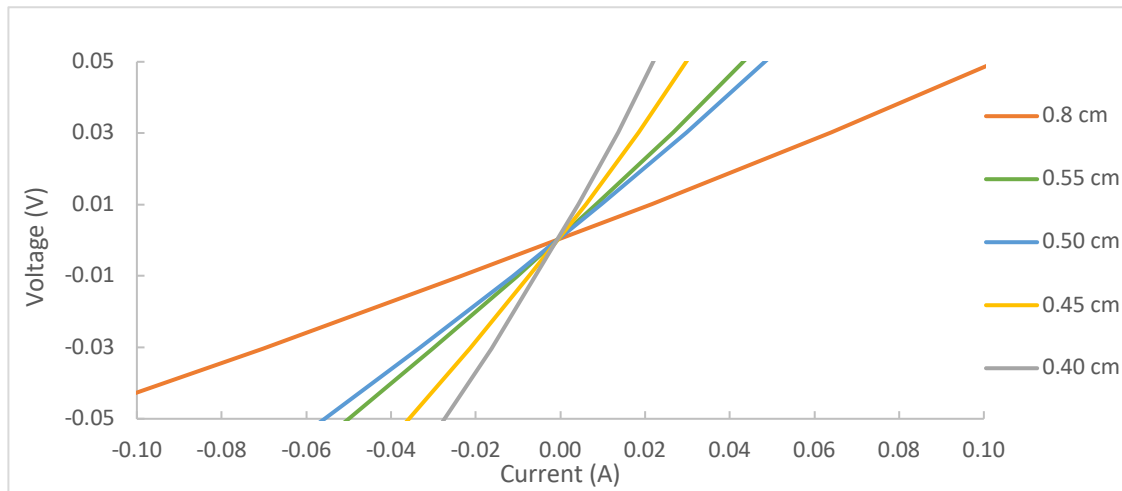
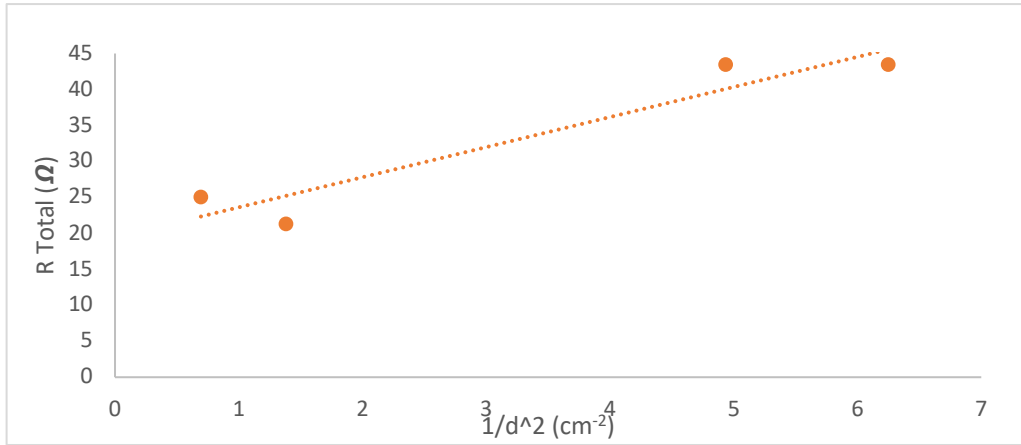


Fig. 11: I-V with C/S: I-V lines for different contact diameters with ITO with C/S method.

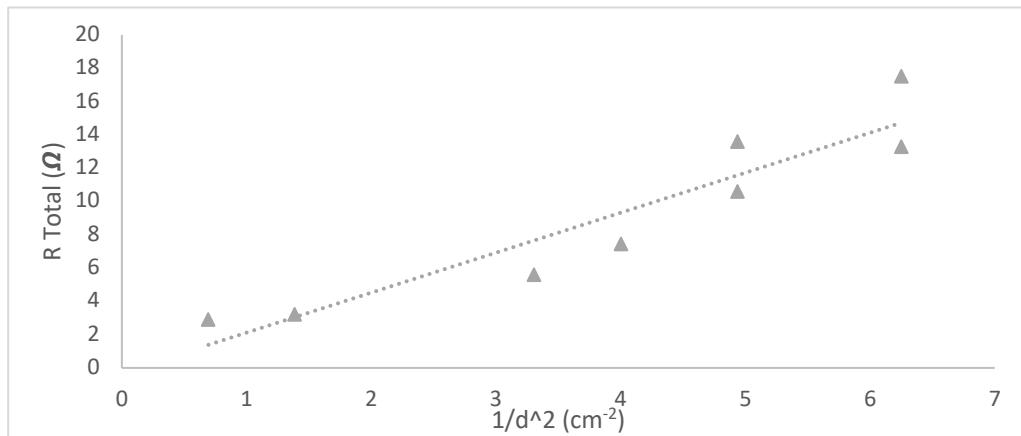
The I-V curves were measured using a different method than the TLM (see methods). This is because the back of the contacts for these samples was uniform (they weren't circles on both sides as seen in Fig. 7). There are linear trends for the voltage versus current from this graph which indicates I can use them to extract the contact resistance from their slope. From this, a graph of the total resistance versus the diameter-squared of the contacts will give me the contact resistivity (see Equation 4). From the slope of Fig. 12, the contact resistivity was extracted. This is the first application of the C/S method for measuring the contact resistance in solar cell prototypes. All the TCO's are shown on the following graphs:

3.2.2 C/S: inverse area total resistance:

(A)



(B)



(C)

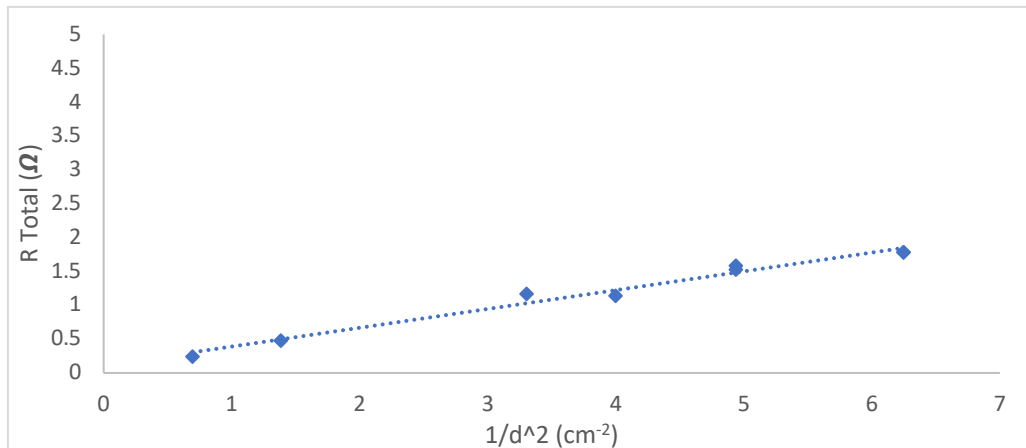


Fig. 12: A-B-C: Total resistance versus the inverse diameter squared of the circular contacts for: IO, IZO, and ITO (in that order) using the C/S method.

To get the contact resistance, the slope was taken from each figure above. ITO and IZO showed the most linear trends and show promise in future experiments. Finally, the analysis of the two different methods for three different TCOs (ITO, IZO, and IO) showed whether the two different measurements agree and whether the new C/S method on solar cells is reproducible on thinner semiconductors.

3.3 Discussion

3.3.1: Comparing the two methods:

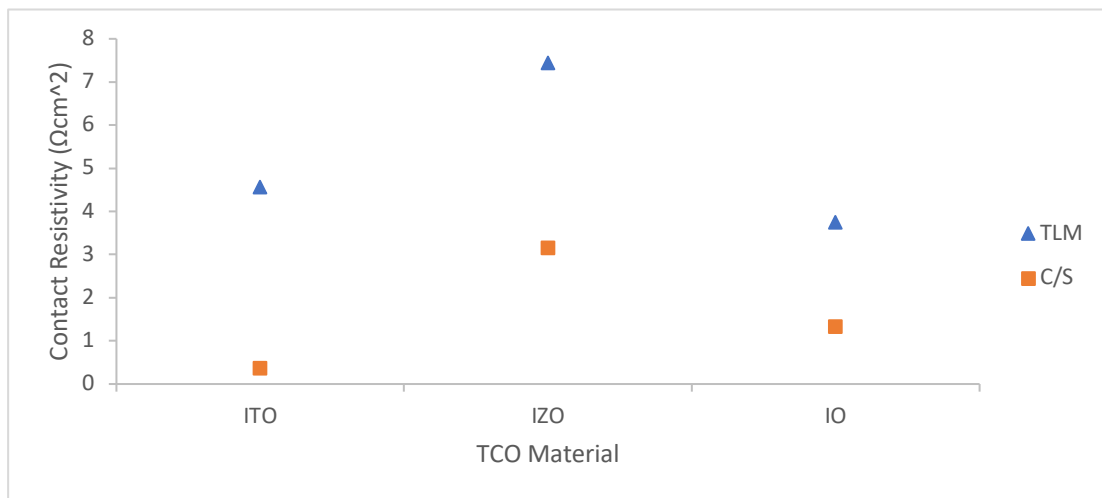


Fig. 13: The contact resistivities for all the different TCO's for the two different measurement methods.

The graphs obtained using the TLM aren't linear, this indicates something went wrong when doing the final measurements. I think two things occurred which affected the results for measuring the contact resistance. First, the samples were lasered out which could have caused the back and front of the sample to meld together. Second, the current and voltage ran through the samples was high (~ 20 V and ~ 1.5 A) when sweeping the I-V curves for the TLM samples. For smaller values of voltage and current I saw linear I-V curves with smaller slopes as expected. The graphs obtained for the C/S method are linear for only ITO and IZO, and less for IO. They agree with previous results gathered by my mentor Will in terms of the contact resistance values. This indicates circular contacts might be used in later experiments with ITO and IZO.

Chapter 4:

Conclusion

The TLM and C/S method have been used to measure the contact resistance for three different TCO's with a n-doped silicon interface. The TLM showed non-linear trends for the total resistance versus pad spacing. This means the standard analytical method for extracting the contact resistance wasn't successful. However, we used data from shortest contact pad spacings to estimate contact resistance.

The C/S method showed linear trends for the inverse area of contacts versus the total resistance, as expected from the C/S model. The contact resistances obtained from the TLM and C/S were different (Fig 13), this means the two methods did not agree. However, C/S method proved to be about a factor of ~ 2 smaller than TLM for IZO and IO. For ITO, the C/S method contact resistivity agreed with my mentor's previous data for TLM. Further research will be necessary with the C/S method to fully understand the perfect dimensions for area of contact, and ideal candidates to be used as TCO's would be ITO and IZO. Since IZO and IO show higher resistance, larger circular pads are suggestive for future trials. Measurements of contact resistance on solar cells with multiple junctions and for thinner semiconductors will help the solar cell industry.

References

- [1] S. Cells and S. Irvine, 1097 (2017).
- [2] D. L. Meier and D. K. Schroder, IEEE Trans. Electron Devices **31**, 647 (1984).
- [3] D. K. Schroder and D. L. Meier, IEEE Trans. Electron Devices **ED-31**, 637 (1984).
- [4] R. H. Cox and H. Strack, Solid. State. Electron. **10**, 1213 (1967).
- [5] S. DeWolf, A. Descoeudres, Z. C. Holman, and C. Ballif, Green **2**, 7 (2012).
- [6] A. Cuevas, Y. Wan, D. Yan, C. Samundsett, T. Allen, X. Zhang, J. Cui, and J. Bullock, Sol. Energy Mater. Sol. Cells **184**, 38 (2018).